Published in "ACS Applied Materials & Interfaces 2(1): 165–174, 2009"
which should be cited to refer to this work.

Stimuli-Responsive Mechanically Adaptive Polymer Nanocomposites

Kadhiravan Shanmuganathan,[†] Jeffrey R. Capadona,[†,§] Stuart J. Rowan,*[,†,§,⊥] and Christoph Weder*[,#,†]

Department of Macromolecular Science and Engineering and Department of Chemistry, Case Western Reserve University, 2100 Adelbert Road, Cleveland, Ohio 44106, Department of Biomedical Engineering, Case Western Reserve University, 10900 Euclid Avenue, Cleveland, Ohio 44106, Rehabilitation Research and Development, Louis Stokes Cleveland DVA Medical Center, 10701 East Boulevard, Cleveland, Ohio 44106, and Adolphe Merkle Institute and Fribourg Center for Nanomaterials, University of Fribourg, CH-1700 Fribourg, Switzerland

ABSTRACT A new series of biomimetic stimuli-responsive nanocomposites, which change their mechanical properties upon exposure to physiological conditions, was prepared and investigated. The materials were produced by introducing percolating networks of cellulose nanofibers or "whiskers" derived from tunicates into poly(vinyl acetate) (PVAc), poly(butyl methacrylate) (PBMA), and blends of these polymers, with the objective of determining how the hydrophobicity and glass-transition temperature (T_g) of the polymer matrix affect the water-induced mechanically dynamic behavior. Below the T_g (~60−70 °C), the incorporation of whiskers (15.1−16.5% v/v) modestly increased the tensile storage moduli (E') of the neat polymers from 0.6 to 3.8 GPa (PBMA) and from 2 to 5.2 GPa (PVAc). The reinforcement was much more dramatic above T_g, where E' increased from 1.2 to 690 MPa (PVAc) and ~1 MPa to 1.1 GPa (PBMA). Upon exposure to physiological conditions (immersion in artificial cerebrospinal fluid, ACSF, at 37 °C) all materials displayed a decrease in E'. The most significant contrast was seen in PVAc; for example, the E' of a 16.5% v/v PVAc/whisker nanocomposite decreased from 5.2 GPa to 12.7 MPa. Only a modest modulus decrease was measured for PBMA/whisker nanocomposite; here the E' of a 15.1% v/v PBMA/whisker nanocomposite decreased from 3.8 to 1.2 GPa. A systematic investigation revealed that the magnitude of the mechanical contrast was related to the degree of swelling with ACSF, which was shown to increase with whisker content, temperature, and polarity of the matrix (PVAc > PBMA). The mechanical morphing of the new materials can be described in the framework of both the percolation and Halpin−Kardos models for nanocomposite reinforcement, and is the result of changing interactions among the nanoparticles and plasticization of the matrix upon swelling.

KEYWORDS: cellulose nanofibers • polymer nanocomposite • biomimetic • mechanically adaptive • responsive

INTRODUCTION

Polymers that change their mechanical properties "on command", i.e., upon exposure to a predefined stimulus in a highly selective and reversible manner, are attractive for countless technologically relevant applications (1). Shape-memory polymers, which have the ability to return from a deformed state to their original shape through a temperature increase (or exposure to other stimuli that cause a temperature increase in the material) represent a design approach that is currently receiving much attention (2). Other classes of widely investigated mechanically adaptable materials include temperature and chemoresponsive polymer (hydro)gels (3), photoresponsive gels (4), liquid crystalline elastomers (5), electrorheological fluids and gels (6), as well as materials that undergo dimensional changes upon stimulation, e.g., electrostrictive (7) materials. Although the mechanical changes of these materials can be quite dramatic—some exhibit viscosity/modulus changes of several orders of magnitude—the large majority of these mechanoresponsive materials exhibits very low moduli (8). Their property profiles are ideal for applications such as drug delivery (9), cell culturing (10), or actuation (7), but examples of much stiffer materials that exhibit such morphing mechanical behavior are limited.

With the objective to develop mechanically adaptive materials for biomedical applications, which upon exposure to physiological conditions slowly (minutes to hours) and without excessive expansion change from a rigid, easily implantable solid to a soft, tissue-matching material, we set out to develop a new family of stimuli-responsive polymer nanocomposites (11) that mimic the function and structural concept of the dermis of sea cucumbers. Like other echinoderms, these creatures have the fascinating ability to rapidly and reversibly alter the stiffness of their inner dermis when threatened (12). Recent studies provided evidence that this dynamic mechanical behavior is achieved through a nanocomposite architecture, in which rigid, high-aspect ratio collagen fibrils reinforce a viscoelastic matrix (13). The stiffness of the tissue is regulated by controlling the interac-

* To whom correspondence should be addressed. E-mail: christoph.weder@unifr.ch (C.W.); stuart.rowan@case.edu (S.J.R.).
Received for review September 17, 2009 and accepted December 2, 2009
† Department of Macromolecular Science and Engineering, Case Western Reserve University.
‡ Department of Biomedical Engineering, Case Western Reserve University.
§ Rehabilitation Research and Development, Louis Stokes Cleveland DVA Medical Center.
⊥ Department of Chemistry, Case Western Reserve University.
Adolphe Merkle Institute and Fribourg Center for Nanomaterials, University of Fribourg.

tions and therewith the stress transfer among adjacent collagen fibrils by locally secreted proteins through either noncovalent (14) or covalent (15) bonds. Intrigued by this capability, we explored synthetic nanocomposites that exhibit similar architecture. A first series of nanocomposites was created from a rubbery ethylene oxide-epichlorohydrin copolymer (EO-EPI) into which a rigid cellulose nanofiber network was incorporated. At ambient temperature, the EO-EPI matrix displays a low tensile storage modulus E' (~4 MPa for a 1:1 ethyleneoxide-epichlorohydrin copolymer) and can accommodate the uptake of several chemical stimuli. Cellulose nanofibers, isolated from the mantles of sessile sea creatures known as tunicates, were used as the reinforcing filler (16, 17). These so-called "whiskers" exhibit high stiffness (tensile modulus ~130 GPa) and dimensions at the nanometer scale (26 nm × 2.2 μm) (18). Similar, albeit shorter nanofibers can be isolated from a range of renewable biosources, including wood (19) and cotton (20). On account of the high density of strongly interacting surface hydroxyl groups, cellulose whiskers have a strong tendency for aggregation (21−23). Good dispersion during processing is achieved when whisker self-interactions are "switched off" by competitive binding with a hydrogen-bond-forming solvent (11). Upon solvent removal, the interactions among the whiskers are "switched on" and they assemble into a percolating network (11). This architecture and strong interactions among the whiskers maximize stress transfer and therefore the overall modulus of the material. Indeed, E' increased with increasing whisker content from ~4 MPa (neat polymer) to ~800 MPa (19% v/v whiskers). We demonstrated that E' of these nanocomposites can be changed through the addition or removal of water, which acts as a chemical regulator and changes the degree of interaction (through hydrogen bonding) between the whiskers within the polymer matrix (as well as presumably the whisker matrix interaction) (11). The uptake of a small amount of water (~30% v/v) causes a large modulus reduction (e.g., from 800 to 20 MPa for a composite comprising 19% v/v whiskers); the original stiffness was restored when the composites are dried. Control experiments and analyses using mechanical models support the conclusion that the stiffness change is primarily a consequence of the designed mechanism of altered whisker−whisker interactions, rather than alternative effects such as plasticization of the matrix (11). Although the mechanical contrast of the EO-EPI/cellulose whisker nanocomposites is remarkable, E' of the most rigid composition studied (800 MPa) was lower than desirable for the targeted use in cortical electrodes (24). We therefore sought to combine the switching mechanism with a chemically influenced thermal transition. We discovered that nanocomposites based on poly(vinyl acetate) (PVAc) and cellulose whiskers display such a "dual" responsive behavior. Upon exposure to physiological conditions (simulated by immersion in water or artificial cerebral spinal fluid, ACSF, at 37 °C), the materials slowly (diffusion control) take up aqueous fluid, which plasticizes the PVAc and reduces the glass transition temperature (T_g) from 42−60 °C (depending on annealing conditions and method of measurement (25)) to ~20 °C, i.e., from above to below physiological temperature. Thus, upon implantation, the matrix effectively undergoes a slow phase transition, changing from a glassy to a rubbery amorphous material. In addition, the whisker−whisker interactions are switched off because of competitive hydrogen bonding with the water. This leads to a dramatic mechanical contrast between the dry state at room temperature (E' = 5.1 GPa for a nanocomposite with 16.5% v/v cellulose whiskers) and the water or artificial cerebrospinal fluid (ACSF) swollen state at 37 °C (~2−12 MPa) (11). Unfortunately, under these conditions the water or ACSF take-up of the reported systems was quite significant (~70−90% w/w for nanocomposites comprising 16.5% v/v whiskers), which may be an impediment for the targeted use in cortical electrodes (24). Our previous data (11) suggest that the swelling behavior of polymer/cellulose whisker nanocomposites depends on several factors, including the whisker surface chemistry and content, temperature of swelling, and polarity of the matrix, but this latter aspect was not systematically investigated. We here report our efforts to gain a better understanding of how the extent of swelling mediates plasticization of the matrix polymer and disengagement of the reinforcing whisker network, to induce dynamic mechanical behavior of these adaptive materials. Cellulose whisker nanocomposites with poly(butyl methacrylate) (PBMA) and PBMA/PVAc blends were employed (Chart 1) because PBMA is more hydrophobic than PVAc, but features a similar T_g (PBMA, 70 °C; PVAc, 42−60 °C). The improved mechanistic understanding of both the thermal and chemical stimuli gained by the present study will be useful for the development of future generations of mechanically adaptive materials aimed at specific applications.

Chart 1

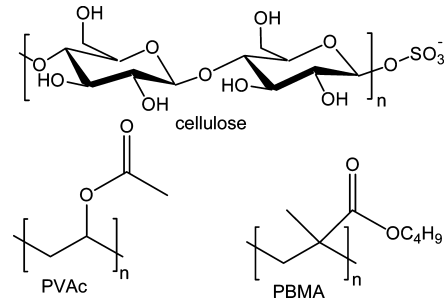

EXPERIMENTAL SECTION

Materials. Poly(vinyl acetate) (PVAc, weight-average molecular weight, M_w = 113,000 g/mol, density, δ = 1.19 g/cm^3) and poly(butyl methacrylate) (PBMA, M_w = 337 000 g/mol, δ = 1.07 g/cm^3) were purchased from Sigma-Aldrich. All other reagents were also purchased from Sigma-Aldrich and were used without further purification. Artificial cerebrospinal fluid was prepared by dissolving the following materials in 1 L of deionized water (26): NaCl = 7.25 g, KCl = 0.22 g, $NaHCO_3$ = 2.18 g, $CaCl_2 \cdot 2H_2O$ = 0.29 g, KH_2PO_4 = 0.17 g $MgSO_4 \cdot 7H_2O$ = 0.25 g, D-glucose = 1.80 g.

Isolation of Cellulose Whiskers. The isolation of cellulose whiskers largely followed our published protocols with minor modifications (22). In brief, tunicates (*Styela clava*) were col-

lected from floating docks at Point View Marina (Narragansett, RI). After gutting, the incrustations on the surface of the tunicates were removed by heating in aqueous potassium hydroxide (3 L, 5% w/w per 500 g of tunicate mantles, 80 °C, 24 h), followed by mechanical agitation, scrubbing, and two more treatments with aqueous potassium hydroxide (3 L, 5% w/w, 80 °C, 24 h); this protocol represents a minor modification of the procedure reported by Yuan et al. (27) After washing the cellulose with water to obtain a neutral solution, we added water (3 L), acetic acid (5 mL), and sodium hypochlorite solution (>4% chlorine, 10 mL), and the temperature was increased to 60 °C. In 1 h intervals, additional portions of acetic acid (5 mL) and sodium hypochlorite solution (>4% chlorine, 10 mL) were added until the material's color changed from pinkish to white. Finally, the bleached deproteinized mantles were washed with deionized water and disintegrated in a Waring blender, yielding a fine cellulose pulp. Sulfate functionalized tunicate whiskers were prepared by sulfuric acid hydrolysis of the cellulose pulp, according to the method described by Favier et al. (28) with slight modifications. Sulfuric acid (98%, 960 mL) was slowly (over the course of 120 min) added under vigorous mechanical stirring to an ice-cooled suspension of tunicate cellulose pulp in deionized water (~6 g in 600 mL, 10 °C). After ~760 mL of the acid had been added, the dispersion was removed from the ice bath and was allowed to warm up to ~40 °C during the addition of the final 200 mL of acid. After the acid addition was complete, the dispersion was heated to 60 °C and maintained at this temperature for 20 min under continuous stirring. The dispersion was filtered through a small-pore fritted glass filter, and the residue was washed with deionized water until the pH increased to at least 5. The residue was subsequently placed into dialysis tubing and dialyzed against deionized water until neutrality was reached. The whisker dispersion was then removed from the dialysis tubing and additional deionized water was added (total volume ~1 L, final whisker content ~8 mg/mL), before the whisker dispersion was sonicated overnight. This dispersion was freeze-dried using a VirTis AdVantage EL-85 lyophilizer with an initial shelf temperature of 25 °C and condenser temperature of −87 °C. The samples were left in the lyophilizer until the vacuum was less than 5 μBar to ensure complete drying and the obtained tunicate whisker aerogel was stored and used as needed.

Preparation of Polymer/Cellulose Whisker Nanocomposites. Lyophilized whiskers were dispersed in dimethyl formamide (DMF) at a concentration of ~5 mg/mL by sonicating for 8−12 h. PVAc, PBMA, or mixtures of these polymers (60:40, 40:60, and 20:80 w/w) were dissolved in DMF at a concentration of ~5% w/w) by stirring for 4−6 h. Nanocomposites comprising 0 − 23.4% v/v whiskers were prepared by combining the appropriate amounts of the cellulose whisker dispersion and the polymer solution, sonication for typically 10 min and casting the resulting homogeneous mixtures into Teflon Petri dishes. The dishes were placed into a vacuum oven (65 °C, 15 mbar, 1 week) to evaporate the solvent and dry the resulting films, before the materials were compression-molded between spacers in a Carver laboratory press (90 °C at 0 psi for 2 min, followed by an increase of pressure to 3000 psi for 15 min) to yield 200−300 μm thin nanocomposite films. Neat PVAc and PBMA reference films were prepared in a similar manner by compression-molding the polymer as received.

Fabrication of Neat Cellulose Whisker Reference Film by Solution Casting. In order to produce reference films consisting of cellulose whiskers only, the lyophilized cellulose whiskers were dispersed in DMF at a concentration of 5 mg/mL by ultrasonication for 8−12 h, and films were produced by casting the resulting dispersion into a Teflon Petri dish, and subsequent solvent evaporation in a vacuum oven (65 °C, 15 mbar, 1 week).

Dynamic Mechanical Analysis. The mechanical properties of the nanocomposites were characterized by Dynamic Mechanical Analysis (DMA, TA Instruments model Q800). Tests were conducted in tensile mode using a temperature sweep method (23 − 90 °C) at a fixed frequency of 1 Hz, and a strain amplitude of 15 μm. All samples were dried in vacuum (65 °C, 15 mbar, 16−18 h) prior to DMA testing (unless swollen materials were measured) or the swelling experiments. To determine the tensile properties of the nanocomposite films in the wet state, we swelled samples in artificial cerebrospinal fluid (ACSF) at 37 °C for 1 week and conducted DMA experiments using the above setup with a submersion clamp, which allowed measurements while the samples were immersed in ACSF; in this case, temperature sweeps were conducted from 23−75 °C. Additional samples were swollen in ACSF at 65 °C for 1 week and were tested while submersed in ACSF.

Swelling Behavior. Prior to DMA testing of ACSF-swollen samples, the degree of swelling was determined gravimetrically by measuring the weight of the samples pre- and postswelling:

$$\frac{\text{mass of wet sample} - \text{mass of dry sample}}{\text{mass of dry sample}} 100 \quad (1)$$

To minimize the error in measuring the degree of swelling, once the wet samples were taken out of water or ACSF, we placed them on paper tissue to wick the water from the surface; the samples were then immediately weighed.

RESULTS AND DISCUSSION

Mechanical Properties of Dry PBMA/Cellulose Whisker Nanocomposites. Nanocomposite films comprising between 0 and 23.4% v/v cellulose whiskers isolated from tunicates and PBMA were produced by solution-casting from DMF and subsequent compression molding (see Experimental Section for details). The thermo-mechanical properties of these materials were established by dynamic mechanical analyses (DMA). DMA temperature sweeps of the dry nanocomposites (Figure 1) reveal a T_g of around 70 °C (maximum of loss tangent, tan δ), which is independent of the whisker content and matches the T_g of the neat PBMA. At ambient conditions (25 °C, i.e., below T_g) the neat glassy PBMA exhibits an E' of ~580 MPa, which decreases significantly to ~1 MPa, if the polymer is heated above T_g to 85 °C. Below T_g, the PBMA/cellulose whisker nanocomposites show a 6-fold increase in the tensile storage modulus: upon introduction of the rigid filler, E' is increased from 580 MPa for the neat polymer to 3.8 GPa for a nanocomposite comprising 23.4% v/v cellulose whiskers. This behavior is typical of rigid polymers reinforced with a rigid filler and is consistent with the behavior observed for other cellulose whisker nanocomposites with glassy matrix polymers (21, 28, 29). A more significant reinforcement effect is observed above T_g, where E' is increased from 1 MPa for the neat polymer matrix up to 1.1 GPa for the nanocomposite with 23.4% v/v whiskers (at 85 °C). The experimental data above T_g match well with the percolation model (vide infra), which is indicative of the formation of a percolating network of strongly interacting cellulose whiskers within a polymer matrix (11, 30). The intensity (I_α) of the DMA loss tangent (tan δ) peak of the nanocomposites (Figure 1b), which reflects a loss of energy due to the relaxation processes in

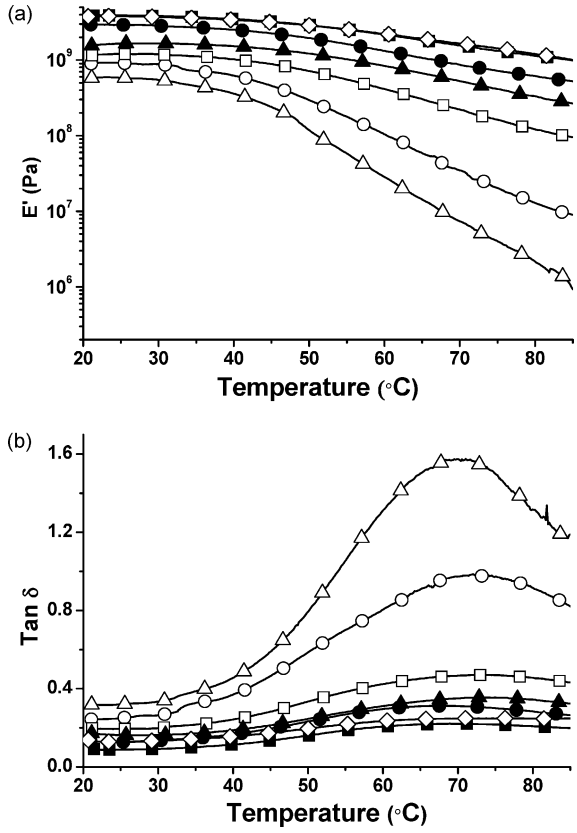

FIGURE 1. Dynamic mechanical analysis (DMA) data of dry films of neat PBMA and PBMA/cellulose whisker nanocomposites as a function of composition. The materials comprise 0 (△), 0.7 (○), 3.6 (□), 7.3 (▲), 11.3 (●), 15.1 (■), or 23.4 (◇) % v/v cellulose whiskers. (a) Tensile storage moduli *E′*. (b) Loss tangent (tan *δ*).

the material and is a measure of the damping behavior, decreases with increasing whisker concentrations. This behavior is similar to that of the PVAc/cellulose whisker nanocomposites and other tunicate whisker reinforced nanocomposites studied before (11, 31) and is indicative of attractive polymer-whisker interactions. Considering the hydrogen bonding opportunities between the PBMA matrix and the hydroxyl-decorated cellulose whiskers, it is likely that the matrix−whisker interactions contribute to the pronounced reduction in magnitude of chain relaxation and hence reduce I_α. The trend does not extend to the 23.4% v/v nanocomposite (I_α is comparable to that of the 15.1% v/v sample), which suggests that the effect levels off at moderate whisker content.

Swelling Behavior and Mechanical Properties of PBMA/Cellulose Whisker Nanocomposites. Our previous study on PVAc/whisker nanocomposites revealed that immersion into water and ACSF (which was used to simulate physiological conditions) led to virtually identical levels of swelling and that the degree of swelling increased with temperature and whisker content (11). With this in mind, and with reference to possible future biomedical applications, we elected to conduct the swelling experiments in ACSF at body temperature. Figure 2 shows the swelling behavior of neat PBMA and PBMA/cellulose whisker nanocomposites at 37 °C. The samples had previously been conditioned by immersion in ACSF at 37 °C for 1 week, to

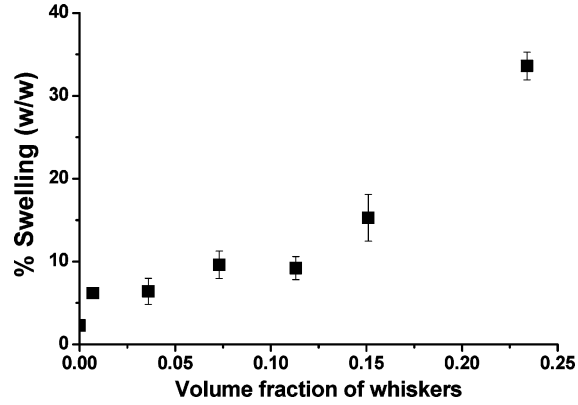

FIGURE 2. Swelling data of PBMA/cellulose whisker nanocomposites as a function of cellulose whisker content. The samples had been conditioned by immersion (to equilibration) in ACSF at 37 °C for 1 week. Data points represent averages ($N = 3-5$) ± standard deviation measurements.

reach equilibrium swelling. Auxiliary data for swelling at 65 °C (i.e., above the T_g of the plasticized PBMA) and reference data for PVAc are compiled in Table 1. Upon swelling the samples expanded isotropically at a level that is commensurate with the water take up. Figure 2 shows that the degree of swelling increased steadily with the whisker content. This effect can be attributed to the increased hydrophilicity of the nanocomposite on account of the presence of the hydrophilic cellulose whiskers. A direct comparison of PVAc and PBMA nanocomposites with similar whisker content (Table 1) reveals that at 37 °C, the latter exhibit—as designed—a much lower level of swelling than the former. For example, the degree of swelling of the PBMA nanocomposite comprising ~15.1% v/v cellulose whiskers is ~15% w/w compared to 75% w/w swelling for the PVAc nanocomposite with similar whisker content.

The thermomechanical properties of ACSF-swollen PBMA-based cellulose whisker nanocomposites, were elucidated by DMA temperature sweeps using a submersion clamp attachment (Figure 3). This set up allowed the samples to remain immersed in ACSF during the mechanical testing, to prevent drying. All samples had been preconditioned by immersion in ACSF at 37 °C for 1 week to reach equilibrium. A comparison with the data of the dry samples (Figure 1) shows that these nanocomposites—very much in contrast to their PVAc-based "cousins" (see Supporting Information, Figure S1, for comparison; the figure is reproduced with permission from ref 11b, copyright 2009 Elsevier)—do not show a very pronounced chemomechanical switching. For example, the modulus of a 15.1% v/v PBMA/cellulose whisker nanocomposite was reduced from 3.8 GPa (25 °C, dry) to 1.2 GPa (37 °C, ACSF-swollen). By contrast, under similar conditions a modulus reduction of almost 3 orders of magnitude (5.1 GPa to 12 MPa) was observed for a 16.5% v/v PVAc/cellulose whisker nanocomposite (11). The data in Figures 2 and 3 reveal that the much lower mechanical contrast of the PBMA nanocomposites upon swelling with ACSF at 37 °C, compared to the previously investigated PVAc/cellulose whisker nanocomposites, has two, somewhat related, origins. As discussed above, the more hydrophobic nature of the PBMA matrix reduces the level of swelling. As

Table 1. Swelling Data of PVAc- and PBMA-Based Cellulose Whisker Nanocomposite Films As a Function of Cellulose Whisker Content and Temperature. PBMA Samples were Swollen in ACSF for 1 Week at the Temperature Indicated; Data Represent Averages ($N = 3-5$) ± Standard Deviation Measurements (indicated in parentheses). Swelling Data of PVAc Nanocomposites in Water Are Reproduced from Reference 11b for the Purpose of Comparison

	swelling of PVAc nanocomposites (w/w %)(11b)			swelling of PBMA nanocomposites (w/w %)	
cellulose whisker content (% v/v)	23 °C	37 °C	cellulose whisker content (% v/v)	37 °C	65 °C
0	4.8 (1.2)	5.8 (3.19)	0	2.3 (0.53)	2.6 (0.86)
0.8	6.5 (0.29)	18.8 (1.53)	0.7	6.2 (0.34)	5.3 (0.68)
4.0	10.4 (2.42)	17.1 (3.00)	3.6	6.4 (1.58)	6.9 (0.89)
8.1	12.2 (1.67)	33.6 (4.70)	7.3	9.6 (1.67)	18.2 (2.86)
12.2	20.2 (2.37)	59.2 (6.48)	11.3	9.2 (1.40)	
16.5	32 (2.69)	75 (12.13)	15.1	15.3 (2.82)	79.5 (4.20)
			23.4	33.6 (1.67)	90.4 (22.14)

a consequence of the low degree of aqueous swelling, the whisker-whisker hydrogen-bond interactions may not be thoroughly "switched off" through competitive binding with water. Equally important is the fact that the plasticization of the PBMA-based nanocomposites upon immersion into ACSF at 37 °C is quite modest: the tan δ vs temperature plots (Figure 3b) show that irrespective of the composition T_g was reduced from ~70 to 50 ±2 °C. This seems to point to a situation where only a small fraction of the water is incorporated as plasticizer into the hydrophobic polymer matrix, while the majority of the water is incorporated around the hydrophilic cellulose whiskers. As a result, at 37 °C the materials are still in the glassy regime, where the PBMA matrix contributes significantly to the overall mechanical properties. This is in stark contrast to the behavior of the PVAc-based nanocomposites, where T_g is reduced from ~60 to 22 °C upon immersion into ACSF at 37 °C. This difference in T_g of PVAc and PBMA in the plasticized state could have also influenced the swelling behavior and the magnitude of the modulus contrast mentioned above. When PVAc nanocomposites are swollen in ACSF at 37 °C, they are well above T_g and hence the higher swelling ratio could be attributed to the increase in free volume above the T_g of the polymer. Because the T_g of plasticized PBMA is around 50 °C, when they are swollen at 37 °C they are still below T_g, which could have led to lower swelling ratio. To confirm this, we did some swelling experiments of neat PBMA and select compositions of the PBMA nanocomposites at 65 °C (15° above the corresponding T_g).

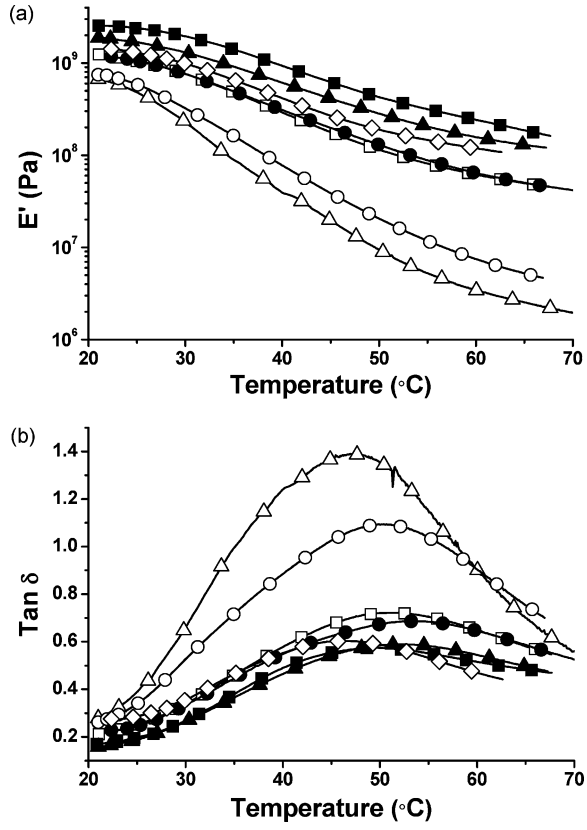

FIGURE 3. Dynamic mechanical analysis (DMA) data of ACSF-swollen films of neat PBMA and PBMA/cellulose whisker nanocomposites as a function of composition: 0 (△), 0.7 (○), 3.6 (□), 7.3 (▲), 11.3 (●), 15.1 (■), or 23.4 (◇) % v/v cellulose whiskers. The samples had been conditioned by immersion in ACSF at 37 °C for 1 week prior to analysis. (a) Tensile storage moduli E'. (b) Loss tangent (tan δ).

As expected, the swelling ratio was much higher at 65 °C compared to 37 °C especially at higher whisker concentrations. For example the swelling ratio of 15.1 % v/v whisker PBMA nanocomposite increased from 15% to 80% (Table 1). This emphasizes the significance of swelling conditions as a critical factor, along with the hydrophilicity of matrix and filler, in determining the degree of water uptake. This experiment also showed that when swollen at 65 °C the PBMA nanocomposite is plasticized (T_g reduced from ~70 °C (dry) to 45 °C) and the modulus at 37 °C is reduced (Figure 4) from 3.8 GPa (25 °C, dry) to 163 MPa (ACSF-swollen at 65 °C). We also observed that, over the entire temperature range (Figure 4), the modulus of the 15.1 % v/v whisker PBMA nanocomposite swollen at 65 °C is much lower than that of the same material swollen at 37 °C. This suggests that in addition to the plasticization effects, higher swelling leads to a more significant disengagement of whisker−whisker (and presumably also whisker-matrix) interactions. However, the fact that the T_g of the matrix is still above the measuring temperature means that the mechanical contrast is not as large as is observed in the PVAc materials. To further understand these systems in more detail, we analyzed the experimental data with respect to two theoretical models.

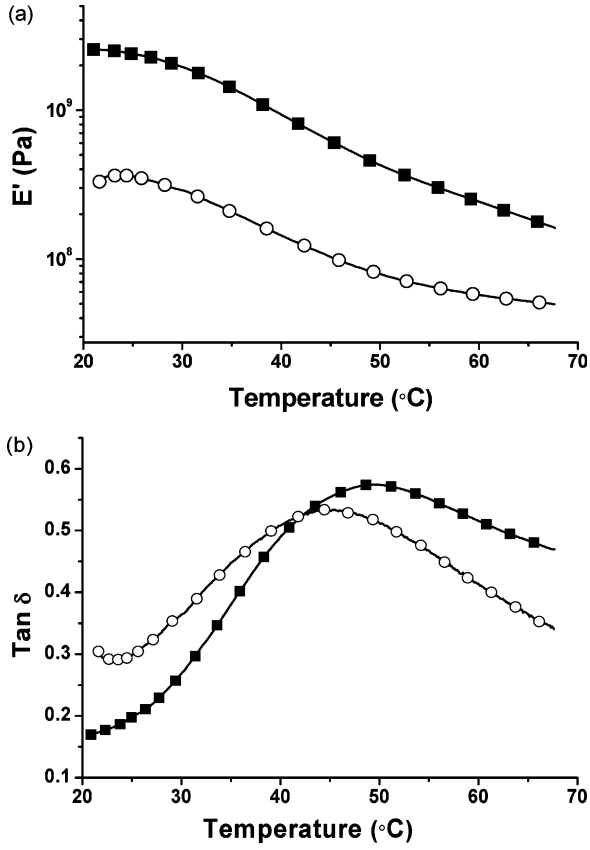

FIGURE 4. Dynamic mechanical analysis (DMA) data of 15.1% v/v PBMA/cellulose whisker nanocomposites conditioned by immersion in ACSF at 37 °C for 1 week (■) or conditioned by immersion in ACSF at 65 °C for 1 week (○). (b) Loss tangent (tan δ).

Discussion of the Mechanical Properties of PBMA/Cellulose Whisker Nanocomposites in the Framework of Limiting Theoretical Models. We have shown before that the mechanical morphing of stimuli-responsive nanocomposites as a result of changing interactions between nanoparticles can be described in the framework of two limiting mechanical models that are commonly used to describe the modulus of nanocomposites of a soft polymer matrix with a high-aspect ratio rigid nanofiller: percolation and mean-field model (11). These descriptions allow one to predict the tensile storage modulus of the nanocomposite E' based on the experimentally determined tensile storage moduli of the polymer matrix and the nanofiller (either an individual filler or a network of fillers, depending on the applied model), E'_s and E'_r, and the volume fraction of the rigid filler, X_r, and dimension (expressed by the aspect ratio, A) of the nanofiller.

Within the scope of the percolation model (eq 2), which was originally used by Takayanagi (32) for semicrystalline polymers and Ouali (33) for phase-separated blends and subsequently applied by Cavaillé for polymer/cellulose nanofiber composites (28, 34), the high-aspect-ratio nanofiller particles are assumed to interact with each other to form a percolating network, and the modulus of the composite is therefore assumed to be governed by this percolating nanofiller network. E' is then given by

$$E' = \frac{(1 - 2\psi + \psi X_r)E'_s E'_r + (1 - X_r)\psi E'^2_r}{(1 - X_r)E'_r + (X_r - \psi)E'_s} \quad (2)$$

It is further assumed that only a fraction of the nanofillers within the nanocomposites contribute to the load transfer, and are defined as ψ (eq 3), which according to percolation theory is

$$\psi = X_r\left(\frac{X_r - X_c}{1 - X_c}\right)^{0.4} \quad (3)$$

given that $X_r \geq X_c$, where $X_c = 0.7/A$ is the critical filler volume fraction needed for percolation (35). By contrast, the Halpin–Kardos model (36) is based on a mean-field approach and predicts E' by

$$E' = 4U_5(U_1 - U_5)/U_1 \quad (4)$$

with

$$U_1 = 1/8(3Q_{11} + 3Q_{22} + 2Q_{12} + 4Q_{66})$$
$$U_5 = 1/8(Q_{11} + Q_{22} - 2Q_{12} + 4Q_{66})$$
$$Q_{11} = E'_L/(1 - \nu_{12}\nu_{21})$$
$$Q_{22} = E'_T/(1 - \nu_{12}\nu_{21})$$
$$Q_{12} = \nu_{12}Q_{22} = \nu_{21}Q_{11}$$
$$Q_{66} = G'_{12}$$

where $\nu_{12} = \phi_r\nu_r + \phi_s\nu_s$; $G'_{12} = G'_s(1 + \eta\phi_r)/(1 - \eta\phi_r)$; $\eta = (G'_r/G'_s - 1)/(G'_r/G'_s + 1)$ and ν is the Poisson's ratio (defined above as 0.3), G' is the shear modulus, and ϕ is equal to the volume fraction of the phase (subscripts r and s refer to the rigid filler and soft polymer phases, respectively). This model assumes that the materials are "quasi-isotropic" and are constituted by many layers of unidirectional plies oriented in alternating directions (−45, 0, 45, and 90°). The properties of the unidirectional reference ply are predicted by the Halpin–Tsaï equations where the modulus in the longitudinal (E'_L) and transverse (E'_T) directs are given by (37)

$$E'_L = E'_s(1 + 2(A)\eta_L\phi_r)/(1 - \eta_L\phi_r) \text{ and}$$
$$E'_T = E'_s(1 + 2\eta_T\phi_r)/(1 - \eta_T\phi_r) \quad (5)$$

where $\eta_L = ((E_{lr}/E_s) - 1)/((E_{lr}/E_s) + 2A)$, and $\eta_T = ((E_{tr}/E_s) - 1)/((E_{tr}/E_s) + 2)$.

This model has been successfully used to describe the modulus of nanocomposites in which the fillers are homogeneously dispersed in a polymer matrix and do not display pronounced filler–filler interactions (37).

We have already shown for EO-EPI and PVAc-based cellulose whisker nanocomposites (11) that the percolation model adequately describes the mechanical properties of the dry nanocomposites, in which the interactions among percolating whiskers are switched "on", whereas the Halpin–Kardos model accurately describes the moduli of these materials when swollen with water or ACSF, i.e., when the filler–filler interactions are switched "off". Figure 5 shows the predictions of percolation (solid line) and Halpin Kardos models (dotted and dashed lines) for the PBMA-based nanocomposites studied here, along with the experimental data for these systems (extracted from Figures 1, 3, and 4). The moduli of the dry PBMA nanocomposites (Figure 5, solid squares) at 85 °C (15 °C above the corresponding T_g, i.e.,

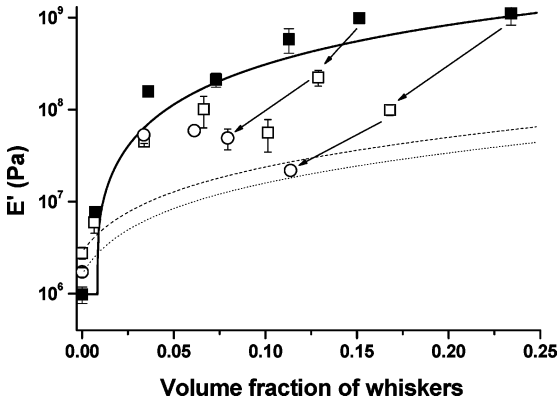

FIGURE 5. Tensile storage moduli E' of neat PBMA and PBMA/cellulose whisker nanocomposites in the dry state at 85 °C (■); ACSF-swollen state at 65 °C after conditioning by immersion in ACSF at 37 °C for 1 week (□); and ACSF-swollen state at 65 °C after conditioning by immersion in ACSF at 65 °C for 1 week (○). Lines show the predictions by the percolation model (solid) and Halpin−Kardos model for samples conditioned in ACSF at 37 °C (dotted) and 65 °C (dashed). Data of ACSF-swollen samples contain a lower volume fraction of whiskers than in their dry state because of solvent uptake. Data points represent averages ($N = 3-5$) ± standard deviation measurements.

in the rubbery regime of the matrix where the assumption that $E'_s \ll E'_r$ holds well) closely follow the prediction of the percolation model, supporting the conclusion that the cellulose whiskers indeed form a percolating network, in which stress transfer among the individual whiskers is facilitated through strong interwhisker interactions. The experimentally determined moduli of the same nanocomposites at 65 °C (15° above corresponding T_g) after they were swollen with ACSF at 37 °C for 1 week (Figure 5, open squares) are significantly reduced compared to the dry materials, but they are higher than predicted by the Halpin Kardos model. Because the T_g of ACSF-swollen PBMA nanocomposites is around 50 °C (which, as discussed above, is lower than that of the dry samples because of plasticization), and that at 65 °C the neat PBMA exhibits an E' of merely ~2.8 MPa, which corroborates the conclusion that the whisker−whisker interactions are only partially switched "off" upon swelling the PBMA-based nanocomposites with ACSF at 37 °C, consistent with a lower water uptake below T_g. However as shown above, swelling the same nanocomposites at 65 °C for 1 week leads to a higher water uptake and the modulus of these nanocomposites falls well below the percolation model, closer to predictions from the Halpin Kardos model (Figure 5, open circles). Although the modulus of neat PBMA is only reduced from 2.8 to 1.7 MPa by swelling at 65 °C, the modulus of the nanocomposites are reduced 4−5 fold. For example, the modulus of a 15.1 % v/v PBMA nanocomposite is further reduced from ~220 MPa to ~50 MPa (measured at 65 °C) when comparing the nanocomposites swollen in ACSF at 37 and 65 °C, respectively. These results are in excellent agreement with the proposed mechanism of extended disengagement of whisker−whisker interactions mediated through increase of the aqueous swelling. Thus under appropriate conditions, the PBMA nanocomposites do exhibit the same switching capability as the PVAc nanocomposites. However, presumably on account of the reduced plasticization of the matrix along with its higher T_g, this switching only occurs at higher temperatures.

We also conducted experiments that probed the reversibility of the switching mechanism for PBMA nanocomposite comprising 23.4 % v/v cellulose whiskers. The materials were swollen at 65 °C for 1 week, subsequently dried in a vacuum oven at 65 °C for 48 h, and the tensile modulus was measured. We found that above T_g, the tensile storage modulus of the nanocomposite after the swelling/drying cycle was similar or slightly higher than that of the control dry nanocomposite (see Figure S4 in the Supporting Information). Below T_g, the modulus dropped slightly from 3.9 to 2.7 GPa. The samples became brittle and opaque possibly due to a solvent-induced morphology change which was also evident in the DSC traces. (DSC thermogram included in the ESI (see Figure S5 in the Supporting Information). Thus, by and large the effect is reversible, as in the previously studied systems, but solvent-induced changes of the matrix morphology appear to be responsible for some hysteresis.

Swelling Behavior and Mechanical Properties of PVAc-PBMA/Cellulose Whisker Nanocomposites. With the objective to create materials that strike a balance between water/ACSF uptake and mechanical contrast, we further investigated cellulose whisker nanocomposites which comprised blends of PVAc and PBMA as the matrix. To limit the parameter space, we kept the cellulose whisker content constant at a level of 11−12 % v/v, whereas we systematically varied the PVAc/PBMA ratio. Like the PBMA/cellulose whisker nanocomposites discussed above, these materials were produced by solution-casting from DMF and subsequent compression molding.

Figure 6 shows the temperature sweeps of dry PVAc, PBMA, and PVAc/PBMA blend nanocomposites comprising between 11.3 and 12.2 % v/v cellulose whiskers. In the high-temperature regime (i.e., above the glass transition), the different materials show rather similar mechanical properties, consistent with the fact that here E' is largely governed by the cellulose whisker network. By contrast, at low temperatures, the E' of nanocomposites that contain little (20 % w/w) or no PVAc is lower than that of nanocomposites which are richer in PVAc. This is consistent with the fact that in the glassy state the modulus of the matrix contributes significantly to the overall stiffness and that the glassy PVAc ($E' \approx 2$ GPa at 25 °C) is much stiffer than PBMA ($E' \approx 580$ MPa at 25 °C).

Figure 7 shows the E' vs temperature and tan δ vs temperature plots of ACSF-swollen cellulose whisker nanocomposites based on the above PVAc, PBMA and PVAc/PBMA blends (after immersion in ACSF at 37 °C for 1 week, i.e., to equilibrium). It is evident from cursory inspection of the graphs that the composition of the matrix has a pronounced effect on the mechanical properties of these ACSF-swollen materials. The entire E' vs temperature curves shift to lower moduli, as the PVAc content is increased. For example, at 37 °C the nanocomposite comprising neat PVAc as the matrix and 12.2 % v/v whiskers displayed the lowest wet modulus of about 12 MPa, while under the same

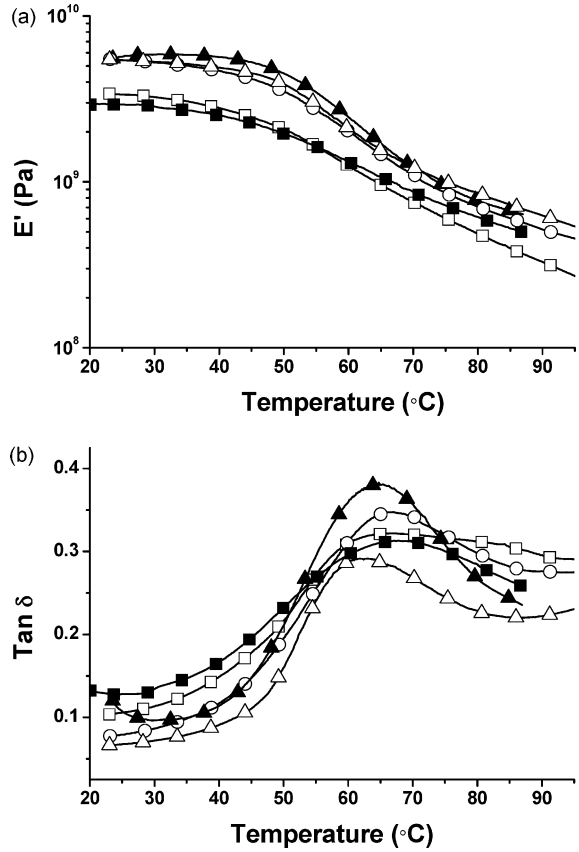

FIGURE 6. Dynamic mechanical analysis (DMA) data of dry films of PBMA-PVAc/cellulose whisker nanocomposites as a function of PVAc/PBMA ratio. The PVAc/PBMA ratio was 100/0 (▲), 60/40 (△), 40/60 (○), 20/80 (□), 0/100 (■); the cellulose whisker content was for all samples between 11.3−12.2% v/v. (a) Tensile storage moduli E'. (b) Loss tangent (tan δ).

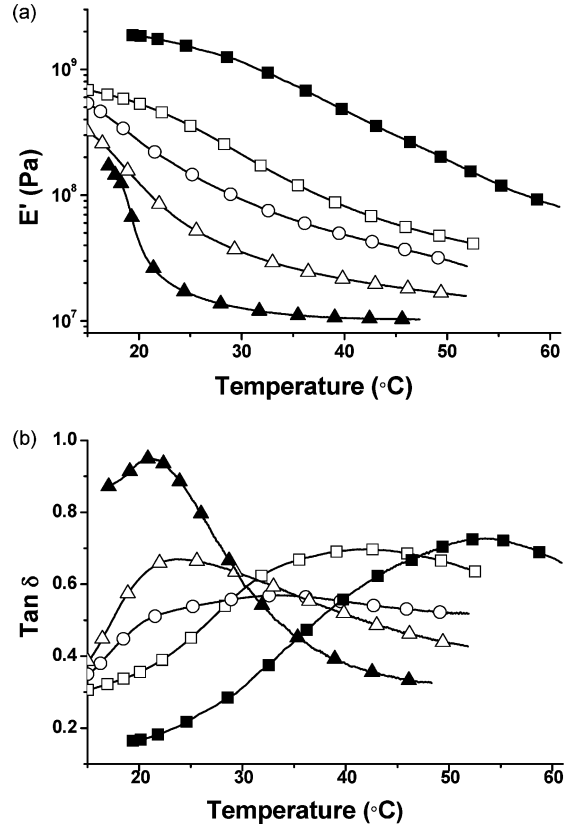

FIGURE 7. Dynamic mechanical analysis (DMA) data of ACSF-swollen films of PBMA-PVAc/cellulose whisker nanocomposites as a function of PVAc/PBMA ratio. The PVAc/PBMA ratio was 100/0 (▲), 60/40 (△), 40/60 (○), 20/80 (□), 0/100 (■); the cellulose whisker content was for all samples between 11.3−12.2% v/v. and the samples had been conditioned by immersion in ACSF at 37 °C for 1 week prior to analysis. (a)Tensile storage moduli E'. (b) Loss tangent (tan δ).

conditions nanocomposite with similar whisker content and a PBMA content of 40, 60, 80, and 100% w/w wet modulus at 37 °C were 24, 57, 100, and 468 MPa, respectively (Figure 7a). The dry moduli of these materials at 37 °C were 5, 4.8, 3.5, and 2.6 GPa respectively. Thus, materials with low PBMA content, display a significant mechanical contrast when comparing the dry materials under ambient conditions with their counterparts that were exposed to (simulated) physiological conditions. Swelling studies of these nanocomposites (Figure 8) demonstrated a steady (but nonlinear) decrease in water uptake with increasing proportion of PBMA in the nanocomposite. A comparison of the mechanical data with the results of the swelling study makes it clear that the wet-modulus of these nanocomposites decreases with the uptake of ACSF. The fact that the shape of the E' vs temperature curves (Figure 7a) also changes with PBMA content is related to the decrease of T_g with increasing PVAc content in the ACSF-swollen materials. This effect is better seen from the tan δ vs temperature plots shown in Figure 7b. The curve of the nanocomposite based on the neat PBMA is quite broad and shows a maximum at ~52 °C, whereas the trace of the nanocomposite comprising only PVAc is more narrow and peaks at ~21 °C. For the materials comprising PBMA/PVAc blends, the peak position is between these extremes and decreases with increasing PVAc content. This explains that the larger switching contrast of the PVAc-

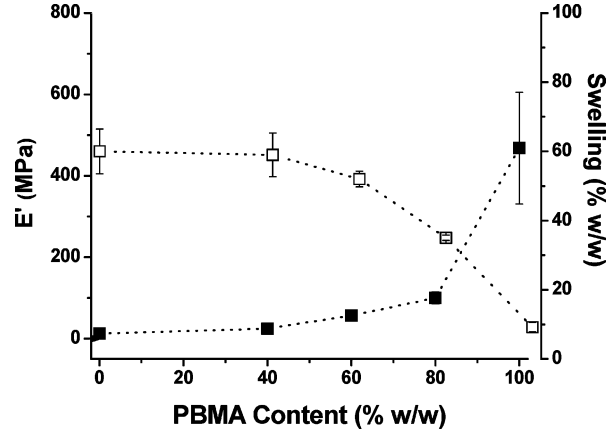

FIGURE 8. Swelling (□) and tensile storage moduli E' at 37 °C (■) of ACSF-swollen PVAc/PBMA based nanocomposite films comprising 11.3−12.2% v/v cellulose whiskers as a function of matrix composition (expressed as PBMA content). The samples had been conditioned by immersion in ACSF at 37 °C for 1 week prior to analysis. Data points represent averages (N = 3−5) ± standard deviation measurements.

rich nanocomposites is related not only to better disruption of whisker−whisker interactions (on account of the higher level of swelling) but also to the fact that plasticization of the PBMA-rich materials is less pronounced, leading to significant matrix contributions to E' at 37 °C. Interestingly, the loss tangent plots of the ACSF-swollen blend nanocompos-

ites feature peaks that appear to be broader than those of the nanocomposites based on either neat matrix polymer (Figure 7b); sometimes the plots reveal two distinct peaks ~21 and ~40 °C (see the Supporting Information, Figure S2). Two distinct peaks (at ~60 and ~80 °C) were also observed for samples that were swollen with ACSF and subsequently dried (see the Supporting Information, Figure S3). This seems to suggest that—at least upon swelling with ACSF—the two matrix polymers actually form a phase-separated blend.

CONCLUSIONS

The objective of this study was to examine how the hydrophobicity and glass-transition temperature of the polymer matrix affect the water-responsive mechanically dynamic behavior of cellulose whisker-based nanocomposites. To this end, PBMA was investigated as the matrix because this polymer is less hydrophilic than the previously studied PVAc, but displays similar thermomechanical characteristics, i.e., a T_g above room temperature. With an eye toward potential applications in the biomedical field, we are particularly interested in the mechanical contrast between films that are dry at room temperature (before implantation) and wet at physiologically temperature (chronic implantation). In contrast to previous observations for nanocomposites of PVAc and cellulose whiskers, where the plasticization with water or ACSF reduces the PVAc matrix T_g to below physiological temperature, placing the PBMA nanocomposites in aqueous solutions (ACSF) at 37 °C results in only a modest T_g reduction to ~50 °C, presumably on account of the higher hydrophobic character of the matrix. Thus, only a small change in modulus is observed between the dry nanocomposites at room temperature versus the swollen nanocomposites at 37 °C (3.8−1.2 GPa for 15.1% v/v nanocomposite), because the matrix remains in its rigid glassy state. Swelling the nanocomposites at 65 °C (i.e., above T_g) causes a significantly higher water uptake (~ 80 vs 15% w/w) and a much lower wet modulus (163 MPa) at 37 °C. This response mirrors the dramatic mechanical contrast observed for the PVAc-based nanocomposites more closely, and suggests that upon swelling above T_g the water is able to induce more decoupling of the whisker network. Furthermore, the modulus of the swollen nanocomposites at 65 °C (i.e., above T_g) is in agreement with theory suggesting that a more complete disengagement of the whisker network does occur. Thus the data show that the T_g and hydrophobic character of the matrix can be utilized to tune the temperature range at which these nanocomposites exhibit their mechanical switching behavior. To further investigate this effect, we also examined how the behavior of the nanocomposite is affected if a blend of both PVAc and PBMA is used as the matrix polymer. The data acquired for a series of nanocomposites with a fixed whisker density but different proportions of PVAc/PBMA revealed that the composition of the matrix blend can be used to control of both the extent of swelling and the chronic wet modulus of the nanocomposites. Thus our investigations of these two systems illustrate how the T_g and hydrophobicity of the polymer matrix can be used to affect the dynamic mechanical behavior of this class of stimuli responsive nanocomposites. The improved mechanistic understanding gained through these experiments will be a useful basis for the development of future generations of mechanically adaptive materials aimed at specific applications.

Acknowledgment. Special thanks to Yuxin Wang for help with lyophilizing cellulose whisker solutions. Financial support from the National Institute of Health under Grant R21NS053798-0, the Case School of Engineering (Ohio Innovation Incentive Fellowship to K.S.), and the Department of Veteran's Affairs Career Development Program (to J.R.C.) is gratefully acknowledged.

Supporting Information Available: Temperature sweeps of dry and wet PVAc-cellulose whisker nanocomposites; loss tangent vs temperature plots of ACSF-swollen and ACSF-swollen and redried films of PBMA-PVAc/cellulose whisker nanocomposites; DMA data illustrating the stiff-soft transition in a 23.4% v/v PBMA/cellulose whisker nanocomposite; DSC thermograms of a dry 23.4% v/v PBMA/cellulose whisker nanocomposite and the same materials after subjecting it to a swelling/drying cycle (PDF).

REFERENCES AND NOTES

(1) Shahinpoor, M., Schneider, H.-J., Eds. *Intelligent Materials*; RSC Press: Cambridge, U.K., 2008.
(2) (a) Lendlein, A.; Kelch, S. *Angew. Chem., Int. Ed.* **2002**, *41*, 2034. (b) Liu, C.; Qin, H.; Mather, P. T. *J. Mater. Chem.* **2007**, *17*, 1543.
(3) de las Heras Alarcón, C.; Pennadam, S.; Alexander, C. *Chem. Soc. Rev.* **2005**, *34*, 276.
(4) See for example: Suzuki, T.; Shinkai, S.; Sada, K. *Adv. Mater.* **2006**, *18*, 1043.
(5) Warner, M.; Terentjev, E. M., Eds. *Liquid Crystal Elastomers*; Clarendon Press: Oxford, U.K., 2003.
(6) (a) Carlson, J. D.; Sprecher, A. F.; Conrad, H. In *Proceedings of the Second International Conference on Electrorhelogical Fluids*; Technomic Publishing Co. Ltd.: Lancaster, PA, 1989. (b) Minagawa, K.; Koyama, K. *Curr. Org. Chem.* **2005**, *16*, 1643.
(7) See for example: (a) Pelrine, R.; Kornbluh, R.; Pei, Q. B.; Joseph, J. *Science* **2000**, *287*, 836. (b) Ebron, V. H.; Yang, Z. W.; Seyer, D. J.; Kozlov, M. E.; Oh, J. Y.; Xie, H.; Razal, J.; Hall, L. J.; Ferraris, J. P.; MacDiarmid, A. G.; Baughman, R. H. *Science* **2006**, *311*, 1580.
(8) Yoshida, R. *Curr. Org. Chem.* **2005**, *16*, 1617.
(9) See for example: (a) Needham, D.; Dewhirst, M. W. *Adv. Drug Delivery Rev.* **2001**, *53*, 285. (b) Peppas, N. A.; Hilt, J. Z.; Khademhosseini, A.; Langer, R. *Adv. Mater.* **2006**, *18*, 1345.
(10) See for example: (a) Shimuzu, T.; Yamato, M.; Kikuchi, A.; Okano, T. *Tissue Eng.* **2001**, *7*, 141. (b) Kwon, O. H.; Kikuchi, A.; Yamato, M.; Sakurai, Y.; Okano, T. *J. Biomed. Mater. Res.* **2000**, *50*, 82–89.
(11) (a) Capadona, J. R.; Shanmuganathan, K.; Tyler, D. J.; Rowan, S. J.; Weder, C. *Science* **2008**, *319*, 1370. (b) Shanmuganathan, K.; Capadona, J. R.; Rowan, S. J.; Weder, C. *Prog. Polym. Sci.* **2010**; DOI: 10.1016/j.progpolymsci.2009.10.005. (c) Shanmuganathan, K.; Capadona, J. R.; Rowan, S. J.; Weder, C. *J. Mater. Sci.* **2010**, *20*, 180.
(12) (a) Heinzeller, T.; Nebelsick, J., Eds. *Echinoderms*; Taylor & Francis Group, London, 2004. (b) Motokawa, T. *Comp. Biochem. Physiol. B* **1994**, *109*, 613.
(13) (a) Trotter, J. A.; Tipper, J.; Lyons-Levy, G.; Chino, K.; Heuer, A. H.; Liu, Z.; Mrksich, M.; Hodneland, C.; Shannon Dillmore, W.; Koob, T. J.; Koob-Emunds, M. M.; Kadler, K.; Holmes, D. *Biochem. Soc. Trans.* **2000**, *28*, 357.
(14) (a) Trotter, J. A.; Koob, T. J. *Matrix Biol.* **1999**, *18*, 569. (b) Sulgit, G. K.; Shadwick, R. E. *J. Exp. Biol.* **2000**, *203*, 1539.
(15) Alberts, B.; Bray, D.; Lewis, J.; Raff, M.; Roberts, K.; Watson, J. D. *Molecular Biology of The Cell*, 3rd ed.; Garland: New York, 1994.

(16) Belton, P. S.; Tanner, S. F.; Cartier, N.; Chanzy, H. *Macromolecules* **1989**, *22*, 1615.
(17) De Souza Lima, M.; Borsali, R. *Macromol. Rapid Commun.* **2004**, *25*, 771.
(18) Sturcova, A.; Davies, J. R.; Eichhorn, S. J. *Biomacromolecules* **2005**, *6*, 1055.
(19) Woodhams, R. T.; Thomas, G.; Rodgers, D. K. *Polym. Eng. Sci.* **1984**, *24*, 1166.
(20) Eichhorn, S. J.; Baillie, C. A.; Zafeiropoulos, N.; Mwaikambo, L. Y.; Ansell, M. P.; Dufresne, A.; Entwistle, K. M.; Herrera-Franco, P. J.; Escamilla, G. C.; Groom, L.; Hughes, M.; Hill, C.; Rials, T. G.; Wild, P. M. *J. Mater. Sci.* **2001**, *36*, 2107.
(21) Capadona, J. R.; van den Berg, O.; Capadona, L.; Schroeter, M.; Tyler, D.; Rowan, S. J.; Weder, C. *Nat. Nanotechnol.* **2007**, *2*, 765.
(22) van den Berg, O.; Capadona, J. R.; Weder, C. *Biomacromolecules* **2007**, *8*, 1353.
(23) Capadona, J. R.; Shanmuganathan, K.; Trittschuh, S.; Seidel, S.; Rowan, S. J.; Weder, C. *Biomacromolecules* **2009**, *10*, 712.
(24) Hess, A.; Dunning, J.; Harris, J.; Capadona, J. R.; Shanmuganathan, K.; Rowan, S. J.; Weder, C.; Tyler, D. J.; Zorman, C. A. Proceedings of the 15th International Conference on Solid-state Sensors, Actuators and Microsystems, IEEE Transducers 2009; Denver, CO, June 21−25, 2009; IEEE: Piscataway, NJ, 2009.
(25) Seyler R. J., Ed. *Assignment of the Glass Transition*; ASTM International: West Conshohocken, PA, 1994.
(26) www.alzet.com/products/cfs_prep.php (accessed 08/04/2009).
(27) Yuan, H.; Nishiyama, Y.; Wada, M.; Kuga, S. *Biomacromolecules* **2006**, *7*, 696.
(28) Favier, V.; Chanzy, H.; Cavaillé, J. Y. *Macromolecules* **1995**, *28*, 6365.
(29) Ljungberg, N.; Cavaillé, J.-Y.; Heux, L. *Polymer* **2006**, *47*, 6285.
(30) Favier, V.; Canova, G. R.; Cavaillé, J.-Y.; Chanzy, H.; Dufresne, A.; Gauthier, C. *Polym. Adv. Technol.* **1995**, *6*, 351.
(31) Dufresne, A. *Compos. Interfaces* **2003**, *10*, 369.
(32) Takayanagi, M.; Uemura, S.; Minami, S. *J. Polym. Sci., C* **1964**, *5*, 113.
(33) Ouali, N.; Cavaillé, J. Y.; Pérez, J. *Elastic Plast. Rubber Comp. Proc. Appl.* **1991**, *16*, 55.
(34) Favier, V.; Canova, G. R.; Shrivastava, S. C.; Cavaillé, J. Y. *Polym. Eng. Sci.* **1997**, *37*, 1732.
(35) Favier, V.; Dendievel, R.; Canova, G.; Cavaille, J. Y.; Gilormini, P. *Acta Mater.* **1997**, *45*, 1557.
(36) Halpin, J. C.; Kardos, J. L. *J. Appl. Phys.* **1972**, *43*, 2235.
(37) Hajji, P.; Cavaillé, J.-Y.; Favier, V.; Gauthier, C.; Vigier, G. *Polym. Compos.* **1996**, *17*, 612.

AM9006337